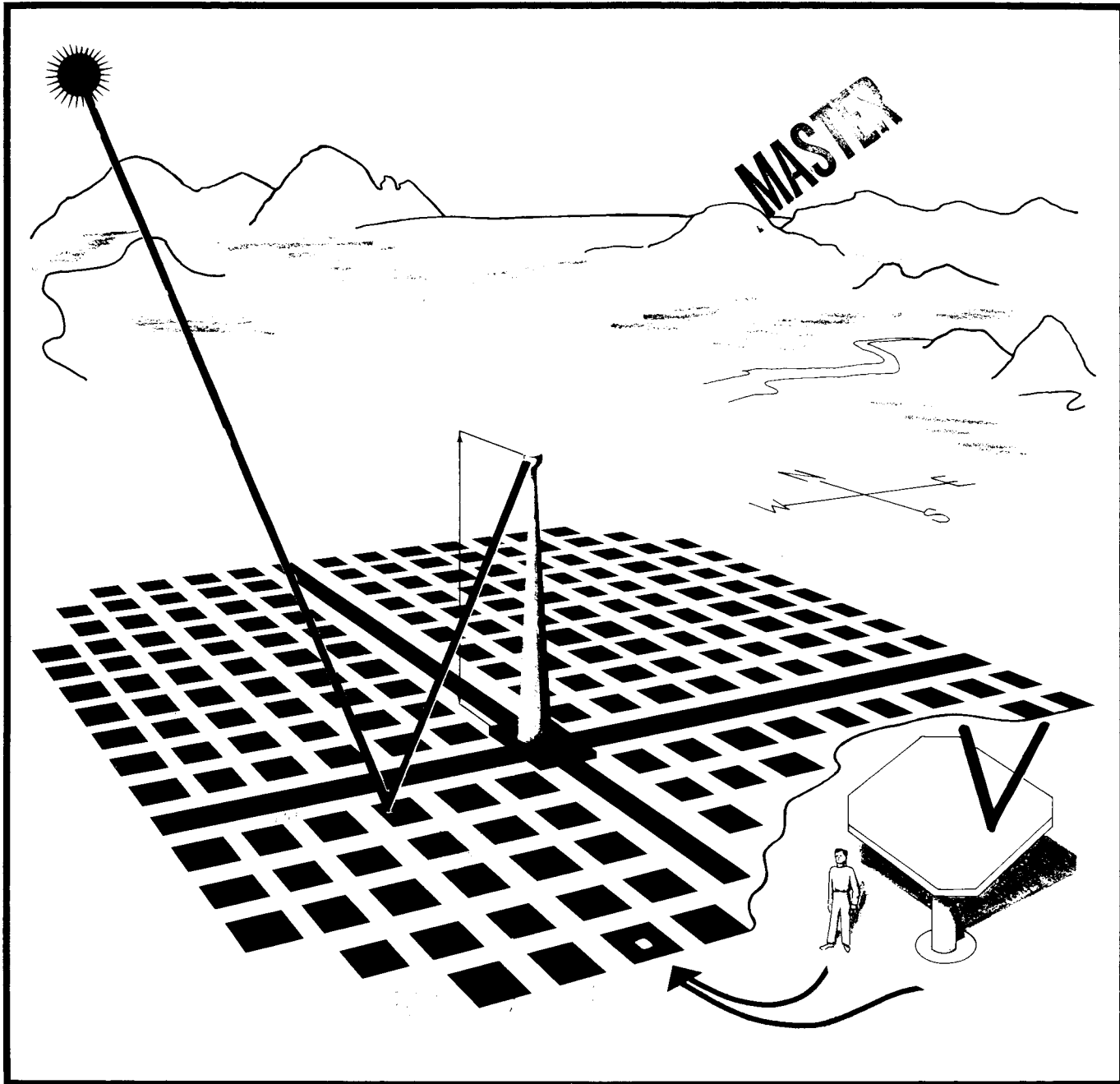


A Description of the Capabilities of the Individual Heliostat Code



A Code Documentation Project
prepared by the
Solar Thermal Division
Energy Laboratory, University of Houston



University of Houston
Houston, Texas 77004

Prepared for the
U.S. Department of Energy
Solar Energy
Under Contract DE-AC03-79SF10763

Solar Energy System Simulation
and Analysis for Central Receiver
Systems

DISCLAIMER

This report was prepared as an account of work sponsored by an agency of the United States Government. Neither the United States Government nor any agency thereof, nor any of their employees, makes any warranty, express or implied, or assumes any legal liability or responsibility for the accuracy, completeness, or usefulness of any information, apparatus, product, or process disclosed, or represents that its use would not infringe privately owned rights. Reference herein to any specific commercial product, process, or service by trade name, trademark, manufacturer, or otherwise does not necessarily constitute or imply its endorsement, recommendation, or favoring by the United States Government or any agency thereof. The views and opinions of authors expressed herein do not necessarily state or reflect those of the United States Government or any agency thereof.

DISCLAIMER

Portions of this document may be illegible in electronic image products. Images are produced from the best available original document.

DISCLAIMER

This book was prepared as an account of work sponsored by an agency of the United States Government. Neither the United States Government nor any agency thereof, nor any of their employees, makes any warranty, express or implied, or assumes any legal liability or responsibility for the accuracy, completeness, or usefulness of any information, apparatus, product, or process disclosed, or represents that its use would not infringe privately owned rights. Reference herein to any specific commercial product, process, or service by trade name, trademark, manufacturer, or otherwise, does not necessarily constitute or imply its endorsement, recommendation, or favoring by the United States Government or any agency thereof. The views and opinions of authors expressed herein do not necessarily state or reflect those of the United States Government or any agency thereof.

**A DESCRIPTION OF THE CAPABILITIES
OF THE
INDIVIDUAL HELIOSTAT CODE**

MICHAEL D. WALZEL

JULY 1980

MASTER

Energy Laboratory
University of Houston
4800 Calhoun
Houston, TX 77004
(713) 749-1154

NOTICE
PORTIONS OF THIS REPORT ARE UNCLASSIFIED
It has been reproduced from the best
available copy to permit the broadest
possible availability.

Prepared for the
U.S. Department of Energy
Solar Energy
Under Contract DE-AC03-79SF10763

ABSTRACT

The individual heliostat, or IH, computer code developed at the University of Houston is available to define heliostat location coordinates of an optimized collector field, and compute in detail the performance of the defined field. In order for IH to generate optimized fields specified by the RC optimization code, IH requires output from CELLAY. CELLAY is a stand-alone program that takes output from the RC system and generates input for the IH programs. A subroutine called LAYOUT and its associated subroutines are the primary source for generating heliostat location coordinates. Boundaries, slip planes, and deletes are all controlled by specification of key variables which occurs before the general sequence of calculations. The IH performance code is similar to the cellwise performance code (NS) with the sum over cells being replaced by a sum over heliostats. Each heliostat has associated with it several quantities which are calculated and output so that the action of the system can be monitored over the course of time. The IH system of computer programs is a collector field layout and performance code for solar central receiver systems.

Acknowledgement

This document was prepared with DOE support under Contract DE-AC03-79SR10763. However, any opinions, findings, conclusions, or recommendations expressed herein are those of the author and do not necessarily reflect the views of DOE. Our working group has developed these codes continuously since June of 1973. Currently this group includes L. L. Vant-Hull, F. W. Lipps, M. D. Walzel, C. Laurence, and A. Holley.

Disclaimer

This report was prepared as an account of work sponsored by the United States Government. Neither the United States nor the United States Department of Energy, nor any of their employees, makes any warranty, expressed or implied, or assumes any legal liability or responsibility for the accuracy, completeness, or usefulness of any information, apparatus, product, or process disclosed, or represents that its use would not infringe privately owned rights. Reference herein to any specific commercial product, process, or service by trade name, mark, manufacturer, or otherwise, does not necessarily constitute or imply its endorsement, recommendation, or favoring by the United States Government or any agency thereof. The views and opinions of author expressed herein do not necessarily state or reflect those of the United States Government or any agency thereof.

TABLE OF CONTENTS

| | Page |
|---------------------------------------------------------------|------|
| Abstract..... | i |
| Acknowledgement..... | ii |
| Disclaimer..... | ii |
| Table of Contents..... | iv |
| List of Figures..... | v |
| List of Tables..... | vi |
| 1.0 INTRODUCTION..... | 1 |
| 2.0 CELLAY..... | 3 |
| 3.0 LAYOUT..... | 10 |
| 3.1 Introduction..... | 10 |
| 3.2 Collector Field Boundaries..... | 11 |
| 3.3 Slip Planes and Deletes..... | 12 |
| 3.4 Specification of Important Controls and Variables..... | 14 |
| 3.5 General Sequence of Calculation..... | 15 |
| 4.0 IH PERFORMANCE CODE..... | 17 |
| 4.1 Heliostat Field Variables..... | 17 |
| 4.2 The Performance Model..... | 19 |
| 4.3 Modes of Operation..... | 26 |
| 4.4 Description of Subroutines Called by YEAR..... | 27 |
| 5.0 CONCLUDING REMARKS..... | 35 |

List of Figures

| | Page |
|------------------|-------------------------------------------------------------------------------------------------------|
| Section 1 | |
| 1-1 | Shading and Blocking Fraction FMIRR for.....4 Individual Heliostats at 3 P.M. on Vernal Equinox |
| 1-2 | Circle-Sector Output of FMIRR Corresponding.....5 3 P.M. on Day of Vernal Equinox |
| 1-3 | North-South Cell Structure.....6 |
| 1-4 | Contour Output for FMIRR Based on Cell.....7 Averages shown in Figure 1-3 |
| Section 3 | |
| 3-1 | Deleted Heliostats and Azimuthal Slides.....13 at the Zone Boundary |
| Section 4 | |
| 4-1 | The Overall Structure of YEAR.....22 |
| 4-2 | The Main Loops in YEAR.....22 |
| 4-3 | Daily Heading and Hourly Summary Outputs.....24 |
| 4-4 | Subroutine Calls in YEAR.....29 |

List of Tables

| | Page |
|-----------|-----------------------------------------------------------------------------------------------------|
| Section 4 | |
| Table 4-1 | List of Heliostat Field.....18 Variables |
| Table 4-2 | List of I/O File Codes.....20 |
| Table 4-3 | List of Files, Subroutines,.....28 and Functions for Individual Heliostat Performance Code |

1.0 INTRODUCTION

In addition to the optimization and performance codes (RC and NS system) developed at the University of Houston, the individual heliostat code (IH) is available to define actual heliostat locations of the optimized field. The IH system will also compute in detail the performance of the defined field. Several output styles exist which allow the user to carefully monitor the efficiency of interaction between the collector field and the receiver.

RC and NS codes are both cellwise in structure. The heliostat field is represented by a regular array of square cells with a north-south and east-west orientation. The cells can be any size and are usually multiples of the tower's focal height. The performance of all heliostats in a cell are represented by a single heliostat at the center of that cell. A group of neighboring heliostats supplied to this representative enable shading and blocking studies on a cellwise basis.

The procedure described above is adequate for conceptual and preliminary optimization and design studies, but a final design mandates a more careful look at the performance of each heliostat surrounded by exactly located neighbors. The accurate representation of the field generated by IH's layout processor is required to represent a true picture of system performance. Only with IH can we deal in an exact manner with discontinuities such as roads, boundaries and internal slip planes.

Primary output required of the RC code to operate the IH code is a set of curve fit coefficients to the heliostat spacing

data delivered to the layout program of IH. These coefficients are generated by a program called CELLAY. Shading and blocking performance data and optimum heliostat spacing data from RC are input to CELLAY. The objective of CELLAY is to produce a set of coefficients for IH which follows, as closely as possible, shading and blocking losses for each region of the RC optimized field. In IH the heliostat array is always radially oriented. Consequently, the local heliostat azimuthal separation is defined by its radial location and is therefore a constrained variable. Spacing coefficients produced by CELLAY for the IH layout routine respond to the constrained azimuth by matching local shading and blocking losses with those of the optimizer (RC). In actuality, heliostat spacings may be somewhat different radially and azimuthally from those reported by the RC code.

The layout routine defines the radii of all circles of heliostats subject to the loss and azimuthal constraints mentioned above. Heliostats are then placed on these circles in a radial-stagger configuration. Heliostats are not allowed on roadways or outside predetermined boundaries. When the azimuthal separation becomes too small because of the decreasing circle radii, a slip plane is defined at which every n^{th} heliostat is removed to relieve the crowding. Heliostats adjacent to the removed heliostat may be moved along their respective circles to minimize any excess shading and blocking that occurs at the slip plane.

Various controls exist to adjust starting and transition points and to remove specified heliostats from the output coordinate files. These controls determine such things as the n^{th}

heliostat to be removed at a slip plane, provisions for determining the radius at which this will occur, and the extent to which heliostats are moved along their circles near a removal.

Once heliostat locations have been defined by the layout processor, a variety of performance calculations and outputs is available. Hourly, daily, and even annual performance can be simulated. Several special studies can be performed. These include startup studies, cloud passage, and emergency defocus operations.

Four output styles are available for field variables such as receiver interception and shading and blocking fractions: (1) individual heliostat output for shading and blocking fractions (Figure 1-1), where output is given by sector, which is the part of a circle between two radii; (2) circle-sector output with circle and sector averages of field variables (Figure 1-2); (3) cellwise output to check overall response compared to the RC and NS systems (Figure 1-3); and (4) contour outputs based on the cellwise output of the field performance variables (Figure 1-4).

2.0 CELLAY

CELLAY is a stand-alone program that takes output from the RC system and generates input for the IH programs. Once the optimization approach of RC has been applied, coefficients are needed to characterize the collector field's optimum heliostat spacings via the IH layout processor. CELLAY requires two matrices of data from the RC programs. One is the number of heliostats located in each cell. The other is the optimal total

SECTOR 8

| | | | | | | | | | | | | |
|-----|------|------|------|------|------|------|------|------|------|------|------|------|
| 2 | 0918 | 0908 | 0908 | 0908 | 0918 | 0911 | 0904 | 0902 | 0897 | 0896 | 0905 | 0895 |
| 3 | 0938 | 0803 | 0980 | 0920 | 0940 | 0792 | 0968 | 0909 | 0941 | 0784 | 0960 | 0902 |
| 4 | 0867 | 0909 | 0959 | 0916 | 0868 | 0898 | 0948 | 0920 | 0871 | 0890 | 0940 | 0945 |
| 5 | 0904 | ** | 0953 | 0864 | 0908 | ** | 0939 | 0853 | 0909 | ** | 0929 | 0873 |
| *6 | 0935 | 0901 | 0925 | 0924 | 0924 | 0924 | 0924 | 0924 | 0928 | 0885 | 0913 | ** |
| 7 | 0927 | 0926 | 0925 | 0925 | 0925 | 0919 | 0925 | 0923 | 0921 | 0919 | 0918 | 0917 |
| 8 | 0926 | 0932 | 0927 | 0923 | 0919 | 0916 | 0914 | 0911 | 0910 | 0909 | 0908 | 0916 |
| 9 | 0937 | 0932 | 0927 | 0884 | 0925 | 0779 | 0921 | 0873 | 0914 | 0922 | 0773 | 0917 |
| 10 | 0792 | 0900 | 0932 | 0926 | 0912 | 0873 | 0889 | 0919 | 0914 | 0875 | 0881 | 0918 |
| 11 | 0873 | 0900 | 0926 | 0884 | 0925 | 0779 | 0921 | 0873 | 0914 | 0875 | 0881 | 0918 |
| 12 | ** | 0916 | 0893 | 0804 | 0873 | ** | 0899 | 0791 | 0870 | ** | 0887 | 0786 |
| *13 | 0942 | 0955 | 0956 | 0856 | 0950 | 0943 | 0947 | 0880 | 0938 | 0934 | 0933 | 0936 |
| 14 | 0954 | 0962 | 0909 | 0934 | 0790 | 0947 | 0945 | 0938 | 0888 | 0934 | 0934 | 0778 |
| 15 | 0911 | 0950 | 0919 | 0878 | 0894 | 0927 | 0937 | 0922 | 0881 | 0881 | 0884 | 0884 |
| *16 | 0954 | 0900 | 0874 | 0844 | 0913 | 0913 | 0901 | 0863 | 0863 | 0959 | 0959 | 0958 |
| 17 | 0922 | 0914 | 0900 | 0769 | 0911 | 0911 | 0923 | 0923 | 0938 | 0938 | 0938 | 0958 |
| 18 | 0889 | 0836 | 0838 | 0902 | 0905 | 0905 | 0890 | 0890 | 0868 | 0916 | 0789 | 0888 |
| *19 | 0910 | 0897 | 0892 | 0886 | 0915 | 0915 | 0945 | 0850 | 0850 | 0981 | 0981 | 0981 |
| 20 | 0936 | 0920 | 0892 | 0887 | 0908 | 0908 | 0908 | 0916 | 0816 | 0919 | 0931 | 0931 |
| *21 | 0929 | 0918 | 0969 | 0921 | 0916 | 0909 | 0921 | 0921 | 0921 | 0922 | 0922 | 0915 |
| *22 | 1000 | 0904 | 0898 | 0896 | 1000 | 1000 | 1000 | 1000 | 0874 | 0874 | 1000 | 1000 |

SECTOR 9

| | | | | | | | | | | | | |
|-----|------|------|------|------|------|------|------|------|------|------|------|------|
| 2 | 0895 | 0907 | 0909 | | | | | | | | | |
| 3 | 0900 | 0951 | 0781 | 0947 | 0902 | 0958 | 1000 | 1000 | 1000 | 0948 | 0899 | 0874 |
| 4 | 0922 | 0884 | 0880 | 0929 | 0939 | 0890 | 0876 | 0926 | 0942 | 0942 | 0924 | 0959 |
| 5 | 0844 | 0920 | ** | 0917 | 0849 | 0929 | ** | 0914 | 0859 | 0942 | ** | 0914 |
| *6 | 0878 | 0927 | 0877 | 0887 | 0933 | 0933 | 0876 | 0897 | 0939 | 0939 | 0877 | 0909 |
| 7 | 0924 | 0925 | 0927 | 0929 | 0930 | 0931 | 0932 | 0933 | 0934 | 0934 | 0935 | 0943 |
| 8 | 0916 | 0918 | 0920 | 0922 | 0925 | 0929 | 0933 | 0933 | 0934 | 0934 | 0935 | 0936 |
| 9 | 0908 | 0908 | 0909 | 0910 | 0912 | 0914 | 0916 | 0920 | 0923 | 0923 | 0927 | 0988 |
| 10 | 0918 | 0773 | 0920 | 0872 | 0920 | 0779 | 0927 | 0882 | 0930 | 0930 | 0791 | |
| 11 | 0919 | 0880 | 0877 | 0916 | 0919 | 0887 | 0875 | 0913 | 0925 | 0897 | 1000 | |
| 12 | 0884 | ** | 0874 | 0791 | 0896 | ** | 0878 | 0805 | 0914 | ** | | |
| *13 | 0863 | 0949 | 0863 | 0879 | 0949 | 0949 | 0863 | 0863 | 0894 | 0894 | 0950 | 0950 |
| 14 | 0935 | 0932 | 0933 | 0933 | 0938 | 0938 | 0947 | 0952 | 0952 | 0957 | 1000 | |
| 15 | 0942 | 0885 | 0937 | 0780 | 0880 | 0936 | 0945 | 0900 | 0953 | 0953 | 0902 | 1000 |
| 16 | 0926 | 0931 | 0889 | 0889 | 0880 | 0856 | 0921 | 0945 | 0945 | 0940 | 0902 | 1000 |
| 17 | 0909 | 0862 | 0917 | ** | 0856 | 0856 | 0857 | 0894 | 0940 | 0940 | ** | 0978 |
| *18 | 0894 | 0909 | 0927 | 0932 | 0915 | 0842 | 0903 | 0894 | 0905 | 0905 | 0978 | |
| 19 | 0944 | 0884 | 0920 | 0915 | 0767 | 0903 | 0892 | 0892 | 0988 | 0988 | | |
| 20 | 0947 | 0914 | 0914 | 0895 | 0882 | 0882 | 0848 | 0833 | 0882 | 0882 | | |
| *21 | 0873 | 0983 | 0946 | 0946 | 0915 | 0915 | 0892 | 0892 | 1000 | 1000 | | |
| *22 | 0947 | 0919 | 0911 | 0898 | 0886 | 0886 | 1000 | 1000 | 1000 | 1000 | | |
| 23 | 0937 | 0915 | 0924 | 0923 | 0824 | 0824 | 0899 | 1000 | 1000 | 1000 | | |
| *24 | 0973 | 0900 | 0880 | 0883 | 0970 | 0970 | | | | | | |
| *25 | 0976 | 1000 | 1000 | 1000 | | | | | | | | |

Figure 1-1. Shading and Blocking Fraction FMIRR for Individual Heliostats at 3 P.M. on Vernal Equinox.

Sectors 8 and 9 are Just North of East. FMIRR is Printed in the Form of a batting Average (i.e., 1000 = 1.0). The ** symbols Mark the place of a deleted Heliostat, and each Twelfth of the Field is Shown Conformally Mapped into a Rectangle: Tower is at the Bottom.

FRACTION OF MIRROR REFLECTING ON THE 0 DAY AT 3.00 HOURS, UNIVERSITY OF HOUSTON

TRUE VALUES= 10 ** 0 X PRINTED VALUES OUTPUT#= 2

| | | | | | | | | | | | | | |
|-----|-------|-------|-------|-------|-------|-------|-------|-------|-------|-------|-------|-------|-------|
| 2 | 0. | 0. | 0. | 0.978 | 0.974 | 0.960 | 0.913 | 0.906 | 0.904 | 0. | 0. | 0. | 0.940 |
| 3 | 0. | 0. | 0. | 0.949 | 0.959 | 0.945 | 0.936 | 0.901 | 0.938 | 0. | 0. | 0. | 0.937 |
| 4 | 0. | 0. | 0. | 0.971 | 0.950 | 0.935 | 0.933 | 0.908 | 0.913 | 0. | 0. | 0. | 0.935 |
| 5 | 0. | 0. | 0. | 0.965 | 0.968 | 0.934 | 0.922 | 0.904 | 0.902 | 0. | 0. | 0. | 0.932 |
| 6 | 0. | 0. | 1.000 | 0.977 | 0.957 | 0.931 | 0.914 | 0.899 | 0.909 | 0.926 | 0. | 0. | 0.932 |
| 7 | 0. | 0. | 0.998 | 0.976 | 0.969 | 0.957 | 0.926 | 0.925 | 0.932 | 0.944 | 0. | 0. | 0.952 |
| 8 | 0. | 0. | 0.999 | 0.961 | 0.962 | 0.950 | 0.935 | 0.922 | 0.927 | 0.943 | 0. | 0. | 0.947 |
| 9 | 0. | 0. | 1.000 | 0.957 | 0.957 | 0.949 | 0.944 | 0.919 | 0.922 | 0.945 | 0. | 0. | 0.948 |
| 10 | 0. | 0. | 1.000 | 0.965 | 0.936 | 0.930 | 0.919 | 0.872 | 0.871 | 0.911 | 0. | 0. | 0.925 |
| 11 | 0. | 1.000 | 1.000 | 0.987 | 0.945 | 0.923 | 0.923 | 0.899 | 0.910 | 0.927 | 0.952 | 0. | 0.941 |
| 12 | 0. | 1.000 | 1.000 | 0.960 | 0.930 | 0.912 | 0.893 | 0.854 | 0.864 | 0.908 | 0.899 | 0. | 0.919 |
| 13 | 0. | 1.000 | 1.000 | 0.972 | 0.938 | 0.928 | 0.911 | 0.899 | 0.902 | 0.938 | 0.934 | 0. | 0.942 |
| 14 | 0.998 | 1.000 | 1.000 | 0.975 | 0.954 | 0.953 | 0.952 | 0.945 | 0.950 | 0.957 | 0.957 | 0.963 | 0.965 |
| 15 | 0.981 | 1.000 | 1.000 | 0.972 | 0.946 | 0.936 | 0.921 | 0.893 | 0.992 | 0.926 | 0.938 | 0.951 | 0.946 |
| 16 | 0.990 | 1.000 | 1.000 | 0.991 | 0.956 | 0.933 | 0.929 | 0.909 | 0.925 | 0.932 | 0.936 | 0.962 | 0.955 |
| 17 | 0.988 | 1.000 | 1.000 | 0.974 | 0.945 | 0.939 | 0.923 | 0.891 | 0.891 | 0.924 | 0.937 | 0.961 | 0.948 |
| 18 | 0.989 | 1.000 | 1.000 | 0.982 | 0.943 | 0.940 | 0.924 | 0.897 | 0.909 | 0.938 | 0.946 | 0.957 | 0.951 |
| 19 | 0.996 | 1.000 | 1.000 | 0.994 | 0.959 | 0.956 | 0.932 | 0.924 | 0.919 | 0.935 | 0.961 | 0.966 | 0.962 |
| 20 | 0.993 | 1.000 | 1.000 | 0.991 | 0.962 | 0.946 | 0.920 | 0.859 | 0.900 | 0.902 | 0.952 | 0.951 | 0.947 |
| 21 | 0.994 | 1.000 | 1.000 | 0.993 | 0.973 | 0.938 | 0.929 | 0.883 | 0.891 | 0.929 | 0.949 | 0.970 | 0.954 |
| 22 | 0.987 | 0.999 | 1.000 | 0.987 | 0.988 | 0.961 | 0.941 | 0.886 | 0.917 | 0.918 | 0.975 | 0.985 | 0.961 |
| 23 | 1.000 | 1.000 | 1.000 | 1.000 | 0.993 | 0.978 | 0.931 | 0.929 | 0.934 | 0.913 | 0.975 | 0.994 | 0.971 |
| 24 | 1.000 | 1.000 | 1.000 | 1.000 | 0.999 | 0.977 | 0.904 | 0.901 | 0.930 | 0.914 | 0.975 | 0.999 | 0.966 |
| 25 | 1.000 | 1.000 | 1.000 | 1.000 | 1.000 | 0.976 | 0.928 | 0.897 | 0.909 | 0.936 | 0.977 | 1.000 | 0.969 |
| 26 | 1.000 | 0.999 | 0.999 | 1.000 | 0.998 | 0.953 | 0.951 | 0.918 | 0.919 | 0.963 | 0.960 | 1.000 | 0.971 |
| 27 | 1.000 | 0.996 | 1.000 | 1.000 | 0.996 | 0.988 | 0.972 | 0.934 | 0.966 | 0.990 | 0.975 | 1.000 | 0.983 |
| 28 | 1.000 | 0.999 | 1.000 | 1.000 | 1.000 | 0.992 | 0.949 | 0.907 | 0.892 | 0.953 | 0.990 | 1.000 | 0.974 |
| 29 | 1.000 | 0.996 | 0.996 | 1.000 | 1.000 | 0.962 | 0.931 | 0.892 | 0.909 | 0.951 | 0.968 | 1.000 | 0.965 |
| 30 | 1.000 | 0.995 | 1.000 | 1.000 | 0.984 | 0.917 | 1.000 | 1.000 | 1.000 | 0.999 | 0.916 | 0.974 | 0.981 |
| 131 | 0.993 | 0.999 | 1.000 | 0.977 | 0.962 | 0.943 | 0.929 | 0.905 | 0.913 | 0.933 | 0.952 | 0.973 | 0.950 |

MAX(A) = 1.0000E 00 MIN(A) = 8.8766E-01 AVR(A) = 9.4962E-01

Figure 1-2. Circle-Sector Output of FMIRR at 3 P.M. on Day of Vernal Equinox.

Right Hand Column Contains Circle Averages. Left Hand Column Contains Circle Numbers. Last Row Contains Sector Averages.

AIJ = (10 ** 0) X PRINTED VALUES

| | | | | | | | | | | | | | | | | |
|-------|-------|-------|-------|-------|-------|-------|-------|-------|-------|-------|-------|-------|-------|-------|----|-------|
| 0. | 0. | 0. | 0. | 0. | 0. | 0. | 0. | 0. | 0. | 0. | 0. | 0. | 0. | 0. | 0. | 0. |
| 0. | 0. | 0. | 0. | 0.958 | 0.955 | 0.949 | 0.961 | 0.938 | 0.924 | 0.912 | 0. | 0. | 0. | 0. | 0. | 0.943 |
| 0. | 0. | 0.972 | 0.960 | 0.928 | 0.939 | 0.943 | 0.939 | 0.924 | 0.922 | 0.917 | 0.913 | 0.915 | 0. | 0. | 0. | 0.932 |
| 0. | 0.974 | 0.966 | 0.959 | 0.956 | 0.945 | 0.942 | 0.949 | 0.928 | 0.928 | 0.919 | 0.907 | 0.894 | 0.893 | 0. | 0. | 0.936 |
| 0. | 0.966 | 0.964 | 0.958 | 0.936 | 0.927 | 0.940 | 0.938 | 0.915 | 0.912 | 0.891 | 0.916 | 0.911 | 0.894 | 0. | 0. | 0.928 |
| 0.969 | 0.957 | 0.970 | 0.956 | 0.939 | 0.943 | 0.950 | 0.951 | 0.912 | 0.909 | 0.893 | 0.893 | 0.915 | 0.902 | 0.906 | 0. | 0.930 |
| 0.943 | 0.965 | 0.962 | 0.956 | 0.959 | 0.972 | 0.979 | 0.977 | 0.912 | 0.895 | 0.900 | 0.888 | 0.908 | 0.903 | 0.990 | 0. | 0.938 |
| 0.981 | 0.965 | 0.968 | 0.977 | 0.989 | 0.997 | 0.989 | 0.958 | 0.933 | 0.919 | 0.894 | 0.906 | 0.909 | 0.913 | 0.921 | 0. | 0.948 |
| 1.000 | 0.993 | 0.996 | 0.996 | 0.999 | 1.000 | 0.998 | 0. | 0.965 | 0.933 | 0.915 | 0.947 | 0.934 | 0.944 | 0. | 0. | 0.967 |
| 0. | 1.000 | 1.000 | 1.000 | 1.000 | 1.000 | 0.998 | 1.000 | 0.967 | 0.954 | 0.940 | 0.923 | 0.923 | 0.944 | 0. | 0. | 0.972 |
| 0. | 0. | 1.000 | 1.000 | 1.000 | 1.000 | 0.999 | 1.000 | 0.984 | 0.957 | 0.941 | 0.921 | 0.934 | 0. | 0. | 0. | 0.977 |
| 0. | 0. | 0. | 1.000 | 1.000 | 0.998 | 0.992 | 0.984 | 0.960 | 0.946 | 0.936 | 0.964 | 0. | 0. | 0. | 0. | 0.974 |
| 0. | 0. | 0. | 0. | 0. | 0.986 | 0.979 | 0.984 | 0.960 | 0.945 | 0. | 0. | 0. | 0. | 0. | 0. | 0.971 |
| 0.970 | 0.970 | 0.976 | 0.975 | 0.974 | 0.975 | 0.973 | 0.965 | 0.940 | 0.929 | 0.915 | 0.913 | 0.914 | 0.911 | 0.940 | 0. | 0.950 |

Figure 1-3. North-South Cell Structure.

Cell Averages of FMIRR Correspond to the Circle-Sector Output of Figure 1-2. The Right Hand and Bottom Outputs Contain Row and Column Averages for the Cells. Note That the Boundary Cells May be Only Partially Occupied.

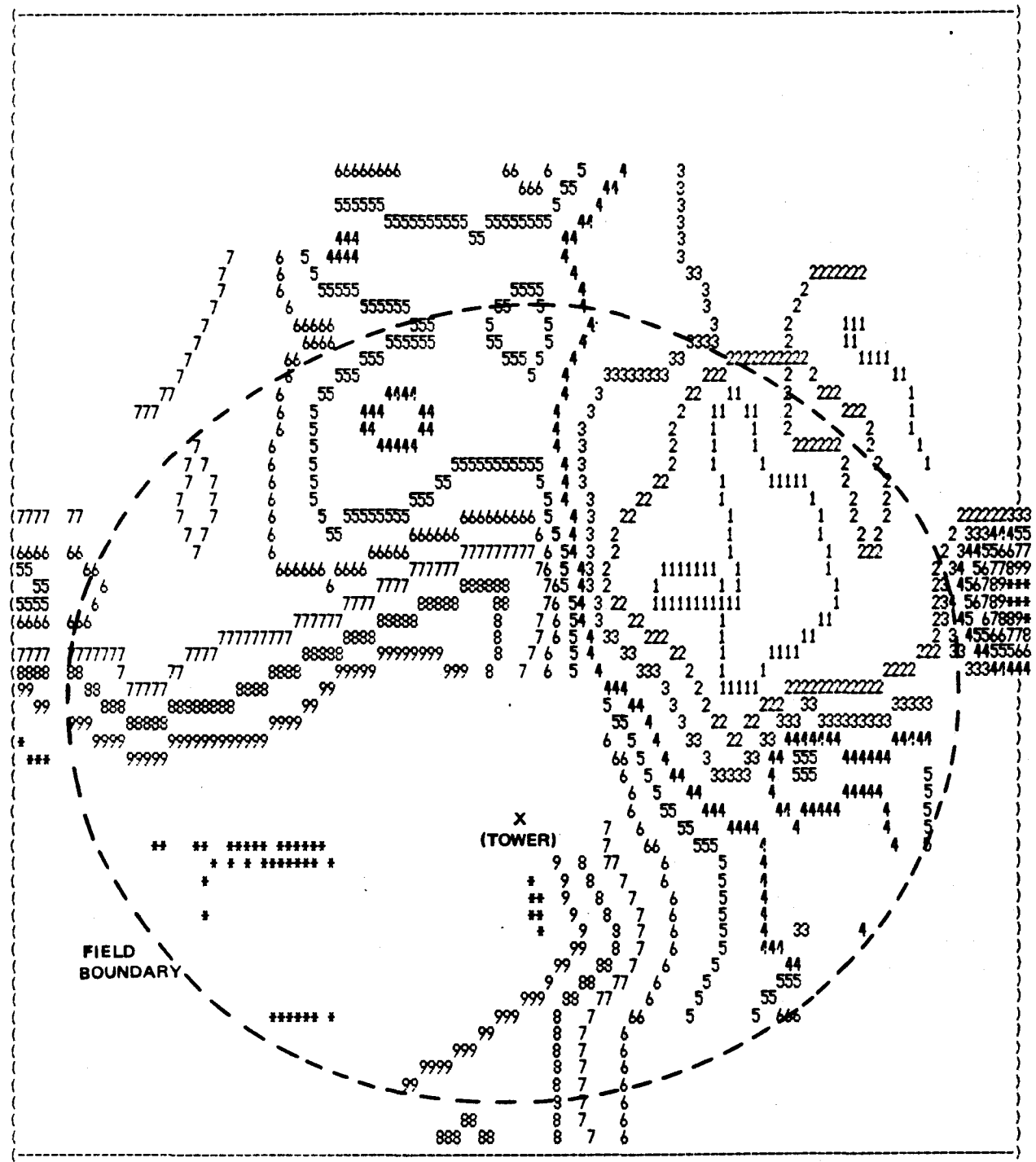


Figure 1-4. Contour Output for EMIRR Based on Cell Averages Shown in Figure 1-3.

In This Diagram the * Represents Unity FMIRR, the 9's Delineate the Region Where FMIRR is = 0.9888, the 8's Delineate the Region Where FMIRR is = 0.9775, etc. The Event on the Right Results From the Fortuitous High of 0.990 on the Right of Figure 1-3, Which is Associated With the 1000's in Circle 3, Sector 9, Figure 1-1.

annual energy redirected per square meter of reflector. This energy matrix has a value in MWH/m² for each cell and takes into account shading and blocking and cosine of incidence losses. In addition, CELLAY uses the shading and blocking data base utilized by RCELL, which contains the losses resulting from 16 different heliostat neighborhoods for each cell. Four azimuthal and four radial spacing are sampled. With this data, four sets of three coefficients are generated for the radial spacing function of IH.

The four sets of coefficients correspond to four different azimuthal spacings sampled by the RC optimizer. In each of the four azimuthal spacings for each cell, a radial spacing is chosen such that the loss due to shading and blocking is identical to the optimum. Thus, for the actual layout in which the azimuthal spacing is constrained by the radial-stagger array, a radial spacing can be chosen such that the annual energy per square meter of reflector is the same as the optimum, even though the spacings are not optimum. Fortunately, optimal azimuthal spacing is everywhere much the same. This means radial and azimuthal spacings are not substantially different from the optimum, although azimuthal spacing changes somewhat.

The idea of four sets of coefficients for radial spacing is an improvement on the prior layout approach that used but one set of coefficients and one polynomial. Previously, in the choice of radial spacing, investigators ignored the fact that azimuthal separation along the arc was becoming smaller within a zone. A zone is a region where all heliostats have the same angular separation as measured from the tower. As one moves

toward the tower from the periphery of a zone, the number of heliostats within a fixed angle of azimuth must be reduced to prevent abnormal azimuthal crowding. When this is done, a slip plane is instituted, the regular array of radial stagger is broken, and a new zone begins. This adjustment of radial spacings in response to the existing azimuthal spacings requires more information than the previous method. CELLAY provides this information by specifying the radial separation required in each cell to give the same shading and blocking loss as we observed in the optimized RCELL run for four specified azimuthal spacings. The four spacings are generally $0.85 Z_0$, $0.95 Z_0$, $1.05 Z_0$, and $1.15 Z_0$, where Z_0 is usually around 2.1 times DMIR. DMIR is the width of the heliostat. All optimum values of Z for the collector field fall within this range of azimuth.

LAYOUT programs use information provided by CELLAY by first determining local azimuthal spacing, which is given (constrained), and then interpolating the four polynomials to find the suitable radial spacing for the particular position in the field determined by the receiver elevation angle. Therefore, the resulting azimuthal and radial spacing shows the same annual cosine of incidence and shading and blocking loss as the optimum RCELL run at the same collector field position (receiver elevation).

3.0 LAYOUT

3.1 Introduction

A subroutine called LAYOUT and its associated subroutines are the primary source for generating heliostat location coordinates. This routine accepts data from the RC system by way of CELLAY to do its job. In addition, data concerning the site, tower and heliostat characteristics are required. Site specifications might include imposed boundaries for the collector field, roads, and slope of the land. Tower focal height (receiver centerline elevation above the plane of heliostat centers) determines field position, and heliostat width and turning radius determine mechanical limits for densest packing. The output of coordinates is given in (X,Y,Z) coordinates, where Z is the vertical distance from the level plane perpendicular to the tower. Polar coordinates are also output.

Heliostats are laid out based upon the radial-stagger neighborhood configuration. In the region near a particular heliostat, the configuration is only slightly compressed azimuthally as the distance to the tower decreases. On the large scale, all heliostats are required to be on circles concentric about the tower. If the ground is sloped, the true circles are in the ground plane and not the level plane. In the level plane they will be elliptical, centered on a point projected from the receiver downward and perpendicular to the ground plane.

The radial stagger layout gives rise to zones within the collector field. These are annular regions where all helio-

stats have the same angular azimuthal separation. In the region of a zone nearest the tower, azimuthal compression is such that a new zone must be started. The number of heliostats per circle is reduced, thereby increasing the angular azimuthal spacing in the new zone nearer the tower. This reduction is typically done with an integer ratio that defines the number of heliostats within a fixed azimuthal range (a sector) in the previous zone compared to the number in the new zone nearer the tower. For the Barstow pilot plant, this ratio was 4/3, which reduces the number of heliostats per circle by 25% each time a new zone is needed.

Currently, only the radial stagger configuration is generated by LAYOUT since this is the configuration recommended by previous RC runs. However, all sizes of fields may be defined, from a few heliostats, to a Barstow-sized plant, to a commercial-sized field. The code, as it exists, defines heliostat coordinates in such a way as to represent in good fashion the RC optimized field. The layout procedure is very fast, and many trial runs can be made at minimal expense. Meanwhile, important control parameters may be varied to utilize information supplied by the RC system so a properly representative collector field may be defined.

3.2 Collector Field Boundaries

There are currently three ways to impose boundaries on a collector field. First, sufficient inputs are available to provide a user defined field boundary, including roads. A second option reads data dumped from an RC run which provides a smoothed

version of the cellwise definition of the field boundary. Third, the user has the option of terminating any circle of heliostats at any angle with respect to a line due south of the tower. These methods give the user flexibility in defining the region in which heliostat pedestals may be placed.

3.3 Slip Planes and Deletes

A slip plane is the region between two zones of the collector field. Slip planes are determined by the code when excessive azimuthal crowding begins to occur within a zone. Deletes are shown by the '*'s in Figure 1-1 and by the X's in Figure 3-1. Deleted heliostats are directly behind heliostats in the next zone. Because blocking would be excessive, they are removed. However, deletions merely result in that particular circle having the same number of heliostats within a fixed sector as the first circle in the new zone. Therefore these deletes actually move the slip plane back one circle. However, we prefer to maintain our definition of the position of the slip plane and acknowledge the deletion of poor performing heliostats.

In Figure 3-1, the solid and dotted circles adjacent to one another in the azimuthal direction show the direction and distance a heliostat is moved along a circle to alleviate excessive blocking. Note that four heliostats are moved toward the deleted position; this intuitively fills the gap and decreases the amount of shading and blocking by giving each moved heliostat more room as well as its neighbors. In the first row of the new zone, two heliostats are moved toward one another to alleviate

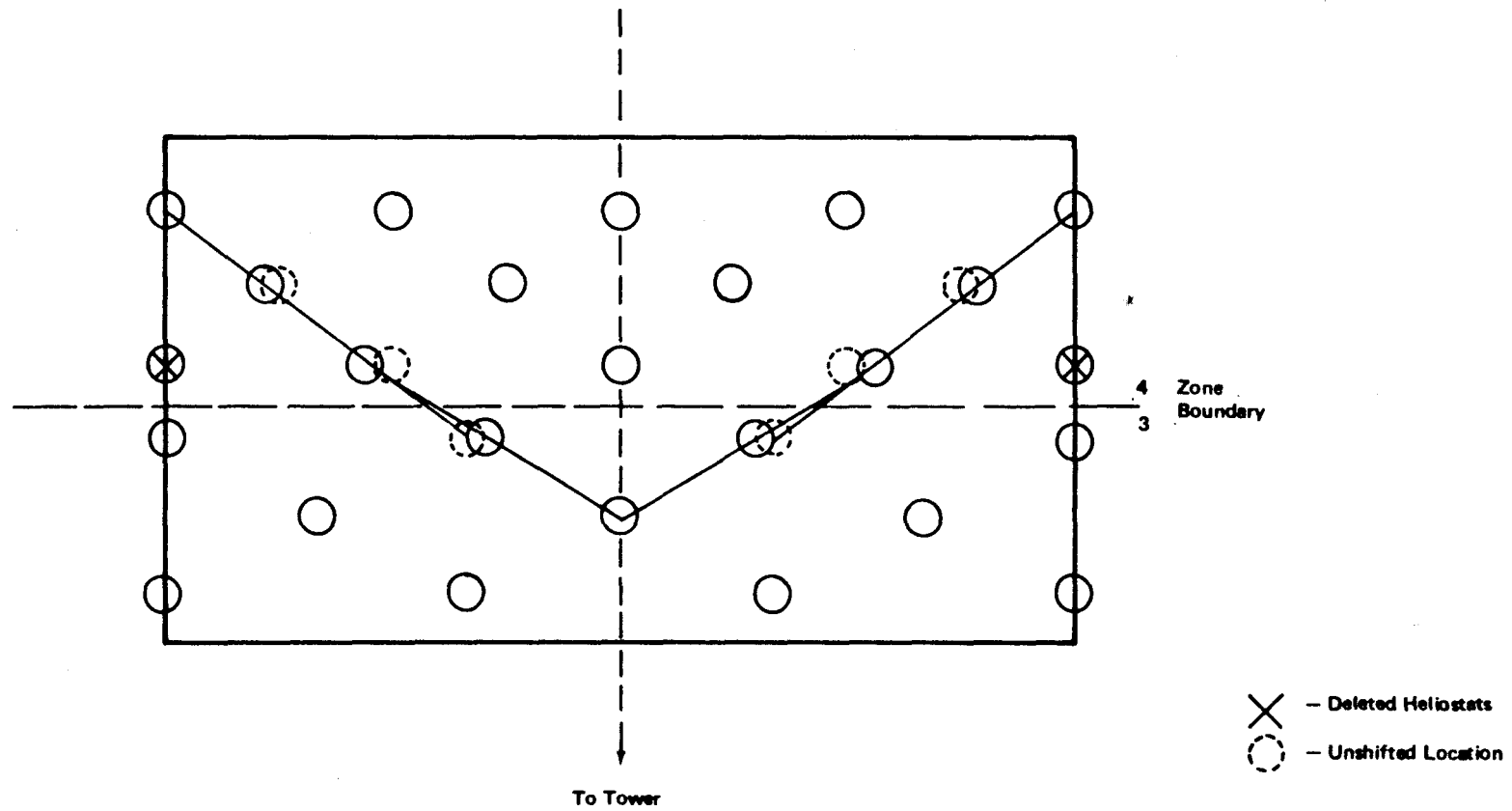


Figure 3-1. Deleted Heliostats and Azimuthal Slides at the Zone Boundary

their blocking heliostats behind them. Here, the azimuthal separation is greater than optimum, so there is no harm in sliding them together. The magnitude of the slides is determined by straight lines drawn diagonally in Figure 3-1. The straight lines ensure that heliostats they connect have equal angular azimuthal separation, thus distributing evenly the blocking loss between heliostats. These adjustments are accomplished by a series of subroutines: CIRCA, CIRCB, etc.

The type of approach just described evolves from studying individual heliostat performance output via the IH programs. By inspection, poorer performing heliostats can be correctly adjusted. Such a remedy helps smooth out and diminish shading and blocking loss in the area of irregular neighborhoods known as the slip plane area.

3.4 Specification of Important Controls and Variables

Four variables input to the LAYOUT subroutine are important in controlling the process of generating heliostat coordinates. These variables can change the look of a particular layout even though the same spacing coefficients are used and the imposed boundaries are not violated. (1) The first variable defines the radius of the outermost circle. This may be user defined or may take its value from imposed boundaries. (2) The second has to do with the azimuthal separation of the outside circle. Changing this variable will alter the location of slip planes within the field. (3) The third control is the minimum azimuthal spacing allowed before a new zone is started. This

variable establishes that lower limit of azimuthal spacings which the azimuthal compression of a zone may not violate. When a violation occurs, a slip plane is instituted. (4) The fourth variable is the zone ratio. It defines the ratio of the number of heliostats contained within a fixed sector for adjacent zones. The zone ratio in Figure 3-1 is 4/3.

These four variables are the important parameters in laying out a field once all data has been received from RCELL, CELLAY, and outside sources. Due to the discrete nature of the generation of the circle radii, an entire circle of heliostats may be lost or gained at the inner boundary of the collector field by slight changes in these variables. Nuances of change can have a substantial effect on the number of heliostats on a specified land area. Therefore, careful "fine tuning" must be done to obtain a desirable layout.

3.5 General Sequence of Calculations

A general breakdown of the operation of LAYOUT will be discussed to reveal the procedure and logic in obtaining a collector field layout. The first item specified by the code concerning the circle radii is the radius of the outermost circle and its azimuthal spacing. Next, CELLAY coefficients determine the radial spacing between the initial circle and the third circle, given the radius and azimuthal spacing of the first circle. The second circle is next placed between the first and third circles using the CELLAY coefficients in a subroutine called HSTEP, which involves an iterative process.

The radii of succeeding circles are generated using this process until a slip plane is encountered. When this occurs, a zone ratio is utilized, and then the radii of the next zone are computed. While this process continues the mechanical limits (the closest distance allowed between adjacent heliostats) are checked at each circle radius which is generated. If mechanical limits are violated, the radius of the new circle is decreased until mechanical limits are satisfied. This process of calculating circle radii continues until the inner boundary of the field is encountered.

After all radii are properly calculated, taking into account the mechanical limits of the heliostats and slip planes, the location of the heliostats on the circles needs to be determined. This only involves the azimuthal placement with respect to the tower since radii are already determined. The placement process considers only the east half of the field since an east-west symmetry for heliostat pedestal positions is assumed. Starting in the north, heliostats are placed along a particular circle according to the subroutine called for that radius. This determines the correct azimuthal spacing along that circle. When we encounter a roadway, we skip heliostats that would normally be placed in that area. This placement process terminates for the circle in question when a boundary is encountered, as discussed earlier.

Roads and boundaries are important limits when we generate a particular heliostat location coordinate. Deletes, slip planes, and slides discussed earlier are taken into account

by the subroutine call for a particular circle radius based on its position within a zone of circles. Many kinds of azimuthal spacings are possible. Four distinct patterns are shown in the example of Figure 3-1. Once the azimuthal placement of all heliostats on a circle is calculated, the (X,Y,Z) coordinates, along with polar coordinates, are written to a data file. The next circle in question is treated in a like manner. Finally, all coordinates are generated and put on file, including the symmetric western half of the field which is generated by a sign change in the Y coordinate of the eastern half of the field. At this point, specific heliostats may be deleted from the list, as desired, by entering their IH defined code number in a function subroutine called ISKIP.

4.0 IH Performance Code

4.1 Heliostat Field Variables

The individual heliostat performance code is similar to the cellwise performance code (NS) with the sum over cells being replaced by a sum over heliostats. Each heliostat has a coordinate vector and a number of special properties. Table 4-1 gives a list of heliostat field variables and a description of properties they represent.

The layout code numbers heliostat circles from the outside to the inside. The outer circle is number one.

Table 4-1. List of Heliostat Field Variables

| <u>Item</u> | <u>Variable</u> | <u>Purpose</u> |
|-------------|-----------------|----------------------------------------------------------------------|
| 1 | XC | X component of heliostat location |
| 2 | YC | Y component of heliostat location |
| 3 | ZC | Z component of heliostat location |
| 4 | AZ | Azimuthal component of heliostat location |
| 5 | FINT | Receiver interception fraction |
| 6 | FCOSI | Cosine of incidence on heliostat |
| 7 | FMIRR | Fraction of useful area after shading and blocking |
| 8 | FAREA | Effective fraction of area (cosine and S and B) |
| 9 | FSAB | Fraction of afternoon insolation weighted FMIRR |
| 10 | ASAB | Annual average of FSAB |
| 11 | ERGM1 | kW/m ² of daily redirected power |
| 12 | ERGM2 | MW/m ² of annual redirected power |
| 13 | RTPOW | Fraction of relative heliostat performance (includes ERGM2 and FINT) |

The first heliostat in the layout is in the outer circle and is the first heliostat east of north. Heliostat number two in the first circle is the symmetric case west of north. Odd numbered heliostats are in the east side of the field, while the even numbered are on the west side. Odd (even) consecutive heliostats are numbered around the circles in clockwise (counter-clockwise) fashion until a circle is filled. The next heliostat is assigned to the first position in the next inner circle. For internal purposes, the IH code lists heliostats in each circle sequentially, clockwise from south.

At present, the layout process is symmetric. Heliostat locations come in east-west pairs regardless of asymmetric boundaries or trim control options. Pairs are written to the output heliostat file consecutively, but they may not be consecutive in the core storage vectors. Asymmetry can be introduced after a symmetric layout by removing heliostats from the set of pedestal locations. This is done by the ISKIP function which allows one to enter a list of heliostats to be removed from each circle. Also, the SUBFLD subroutine limits the effective field to an arbitrary circle-sector region. Thus the actual set of heliostats transmitted to the performance model is the total list of heliostat locations minus a list of removed heliostats.

4.2 The Performance Model

The individual heliostat performance code is similar to the cellwise performance code with two important exceptions:

Table 4-2. List of I/O File Codes

| <u>Code</u> | <u>File</u> | <u>Subroutine</u> |
|-------------|---------------------------------------------|-------------------|
| 05 | System Standard Read File | |
| 06 | System Standard Write File | |
| 09 | AIMS - Aim points from cellwise program | AIM |
| 10 | HELIOS - Coordinate Data | AIM |
| 11 | PLOTD - Circle/sector data for plotter | CIRSEC |
| 14 | NODE1 - Receiver Interception Data | FINTP1 |
| 24 | NODE2 - Receiver Interception Data | FINTP2 |
| 30 | CARD.F - Data to be card punched | PANPOW |
| 38 | Temporary Random File for Helios Panel Sums | FINTP1 |
| 39 | Temporary Seq. File for PANPOW versus TIME | FINTP1 |
| 40 | Temporary Seq. File for Cellwise Panel Sums | FINTP1 |

1. Representative heliostats of the cellwise model are replaced by a complete set of heliostats. Cell structure is restored for certain output purposes by averaging the appropriate heliostat variables.
2. The receiver model is not available in the individual heliostat code, and receiver information is input via the node file and the aims file.

Table 4-2 lists all the input/output files and the subroutine from which they are accessed. Subroutines listed here are described in Section 4.4. The AIMS file inputs aiming strategy data which are produced by the receiver subroutine in the cellwise system. This array of data is interpolated to the individual heliostats and written to the HELIOS file. AIMS data cannot be used in any other way. Other I/O files will be discussed under the appropriate subroutines which access them in Section 4.4.

The IH performance code is contained in the subroutine YEAR. YEAR divides into three phases (Fig. 4-1). Time dependence occurs only in the second phase which is called the diurnal phase. Details of each phase are shown in Figure 4-2, which shows the major loops occurring in YEAR, including the call to the shading and blocking subroutine SAB3. The occurrence of outputs is also indicated.

Output from the initial phase of YEAR is only for FINT. A variety of output options are available. SECTOR can provide a FINT output for each heliostat although this is usually

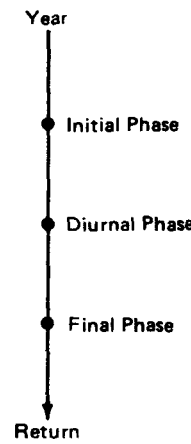


Figure 4-1. The Overall Structure of YEAR

INITIAL PHASE
 LOADS AND OUTPUTS FINT
 INITIALIZES SUBLD IF DESIRED

DIURNAL PHASE
 (DAILY HEADING)
 700 LOOP FOR DAYS
 600 LOOPS FOR HOURS
 (INSULATION MODEL)
 500 LOOP FOR CIRCLES IN COLLECTOR FIELD
 501 LOOP FOR HELIOSTATS IN CIRCLE
 (HELIOSTAT ORIENTATION)
 CALL SAB3 FOR SHADING AND BLOCKING
 501 CONTINUE
 500 CONTINUE
 (HOURLY OUTPUTS)
 600 CONTINUE
 (DAILY OUTPUTS)
 700 CONTINUE

FINAL PHASE
 ANNUAL OUTPUTS

Figure 4-2. The Main Loops in YEAR

not desired. CELTUR can provide an array of cellwise averages for FINT with or without a contour map. CIRSEC can provide an array of circle-sector averages for FINT with or without an additional output to a file for plotter applications.

The first output in the diurnal phase is the daily heading, and the last output of the diurnal phase is an hourly summary. Figure 4-3 provides examples of daily heading and hourly summary outputs. Format for these outputs is identical to that used in the NS performance code.

Diurnal phase outputs are given below. Except for items 4 and 5, all of these outputs are available in the full range of output styles as described for the FINT vector. The basic information output is the same as output in the NS performance code, although individual heliostat values are now available, as well as cellwise averages.

- 1) Fraction of Mirror Reflecting = FMIRR
- 2) Cosine of Incidence Angle = FCOSI
- 3) Effective Fraction of Mirror = FAREA
- 4) Hourly Summary Output
- 5) Elapsed CPU Time
- 6) Afternoon Insolation Weighted Average of FMIRR = FSAB
- 7) Daily Total kWh/m^2 Reflected = ERGM1
- 8) Daily Relative Total Power = RTPOW
- 9) Annual Afternoon Insolation Weighted Average of FMIRR = ASAB
- 10) Annual Total MWh/m^2 Reflected = ERGM2

ON THE 92ND DAY AFTER VERNAL EQUINOX
EARTH = 0.10163220E 01 ASU
SOLAR ELEVATION AT NOON = 78.4407 DEGREES
DAY = 14.3565 HOURS
SUNRISE AZIMUTH = 117.1763 DEGREES

AT 5.000 HOURS THE SUN GIVES
860.224 WATTS/M2. THE TOWERTOP COLLECTOR HAS
3356.014 M2 OF EFFECTIVE AREA AND PROVIDES
2.887 MEGAWATTS OF DIRECTED POWER

| HOURS | USUNX | USUNY | USUNZ | ESUN | ZSUN |
|-------|------------|------------|----------|---------|----------|
| 5.000 | - 0.144261 | - 0.906217 | 0.397441 | 23.4183 | -99.0450 |

Figure 4-3. Daily Heading and Hourly Summary Outputs.

The length of day and azimuth of sunrise refer to the input elevation of startup.

11) Annual Relative Total Power = RTPOW

The final phase outputs are as follows:

- 1) Annual Summary of Insolation,
- 2) Annual Summary of Cosines,
- 3) Annual Summary of FMIRR,
- 4) Annual Summary of FAREA,
- 5) Annual Summary of Receiver Power,
- 6) Annual Summary of System Efficiencies,
- 7) Annual Summary of System Efficiencies/COSI, and
- 8) PANPOW and PANEFF Outputs.

The last executable statement in YEAR calls the PANPOW subroutine which, in turn, calls the PANEFF subroutine.

The PANPOW subroutine and the PANEFF subroutine produce the following outputs:

- 1) Annual Summary of Incident PANEL Power in MW/panel
- 2) Annual Summary of Absorbed PANEL Power in MW/panel
- 3) Annual Summary of System Efficiencies
- 4) Annual Summary of System Efficiencies/COSI
- 5) Annual Summary of Dimensionless Panel Gradients
- 6) Annual Summary of Receiver Asymmetry Ratios
- 7) Annual Summary of Panel MAXIMA in MW printed above Panel Number of the MAXIMA
- 8) Annual Summary of Panel MINIMA in MW printed above Panel Number of the MINIMA
- 9) Annual Summary of Incident Panel Power for a constant direct beam intensity at all time. The nominal intensity is 950 W/m^2 .

- 10) (Same for Absorbed Panel Power)
- 11) Annual Summary of system Efficiencies for a constant direct beam intensity at all times (nominally 950 W/m^2) - Losses Accounted For
- 12) Annual Summary of System Efficiencies/COSI for a constant direct beam intensity at all time (nominally 950 W/m^2) - Losses Accounted For

If PANPOW is called, previous system efficiency outputs do not occur since they would be redundant. Annual summary outputs normally include seven days with seven output times per day. The times begin at noon and end at an input elevation angle which represents a reasonable shutoff condition. Times are equispaced from noon to shutoff. Days are equispaced from summer solstice to winter solstice. However, any selection of time can be studied. Outputs for the seasonally symmetric days can easily be generated by applying a small correction to the insolation.

4.3 Modes of Operation

This section describes applications which are anticipated for the IH code system. At the risk of repetition, it should be mentioned that RCELL provides coefficients for an optimized layout. The IH code does not contain the economic model and does not optimize. Furthermore, the cellwise code writes the node file and the aims file which are read by the IH code when receiver interception, receiver panel power, receiver flux density, and the aiming strategy are required. Typically, a cellwise receiver run and an RCELL optimizer run would be required before starting an individual heliostat study.

Generally, one expects to make a series of layout runs prior to a detailed performance study. The layout process is quite fast and adjustments can be made in the zonal structure, and the approach to various boundaries. As soon as a reasonable preliminary layout is obtained, one should operate the IH code to get the total receiver power at the design time. This requires a node file and the use of the shading and blocking subroutine. If total thermal power is higher than specified, the requirement can be achieved by removing an appropriate number of heliostats from the existing layout or by generating a new, less dense layout. If receiver power is too low, a denser layout may be required. Having achieved the specified total thermal power, the operator deals with the next problem concerning flux density distribution and time dependence of the panel powers. Appropriate subroutine outputs are available and again modifications in layout may be required. If all design requirements are satisfied, the various outputs can be used to predict performance and to analyze the quality of the design.

4.4 Description of Subroutines Called by YEAR

Table 4-3 lists all subroutines and functions which occur in the individual heliostat performance code. Figure 4-4 shows every call which occurs directly in YEAR. The LAYOUT subroutine calls subroutines and functions listed under files INPUT and LAY of Table 4-3. The uses of these subroutines are

Table 4-3. List of Files, Subroutines, and Functions for Individual Heliostat Performance Code

| <u>Files</u> | <u>Subroutines</u> | <u>Functions</u> |
|---------------|------------------------------------------------------------------------------------------------------------------------------------------------------------|------------------------------------|
| INPUT | MAIN LSQF* VALF* | ISKIP RSFC, POLYNM, TRFC, HSTEP |
| LAY | LAYOUT ZONE MECHLM COORDS CIRCA CIRCG CIRCH CIRCI AIM (AIM1) ⁺ DATIM ⁺⁺ AIM2 WREAD TRIM ROADS | |
| YEAR RSABS | YEAR SAB3 EVENT FINTP1 (FINTP3) TOOPAN (COMBO) HINT (CSPANL) | |
| FIELD | CELTUR CIRSEC SECTOR SECPRT ASKPRT SUBJLD ACONTR (VCONTR) | |
| ANNUAL | SUMIT RELPOW PANPOW PANEFF | |

*IMSL subroutines.

+Items in parenthesis are entry points.

++System subroutine for date and time.

Year

- FINTP1(FINT)
- CELTUR(FINT)
- SECTOR(FINT)
- SUBFLD

```

DO 700 NDAY = 1, JMAX
DO 600 IHOR = 1, IMAX
DO 500 IMIR = IROW1, IROW2
DO 501 JMIR = 1, NR

501 CONTINUE ● SAV3(FMIRR)
● CELTUR(FMIRR)
500 CONTINUE ● SECTOR(FMIRR)
● CELTUR(FCOSI)
● CELTUR(FAREA)
● FINTP3
● SUMIT

600 CONTINUE
● CELTUR(FSAB)
● SECTOR(FSAB)
● SUMIT(ERGM1)
● RELPOW

700 CONTINUE
● CELTUR(ASAB)
● SECTOR(ASAB)
● SUMIT(ERGM2)
● RELPOW
● ANNUAL SUMMARY OUTPUT
● PANPOW

RETURN

```

Figure 4-4. Subroutine Calls in YEAR.

SUMIT and RELPOW also call CELTUR and SECTOR for output purposes. CELTUR calls CIRSED and VCONTR for additional outputs.

discussed in Section 3. The subroutine YEAR involves all other subroutines listed under files RSABS, FIELD, and ANNUAL in Table 4-3; those of particular interest are described below.

FINTP1 reads the receiver interception data from the cellwise performance model. These data are contained in the so-called "node file" and are read from file code 14. Panel interception fractions are formed and written to file code 40. Subroutine HINT is called to interpolate receiver interception fractions for individual heliostats. HINT also has an option to interpolate panel fractions. Panel fractions are converted to panel powers and written to file code 39. COMBO is called if a blend of aiming strategies is required.

TOOPAN and COMBO are used to blend node files representing different aiming strategies. There may be two node files: one file for a two-point aiming strategy and a second file for a one-point aiming strategy. It may happen that neither the one-point, nor the two-point aiming strategy can produce a satisfactory flux density profile, but a blend of the two strategies may be satisfactory. TOOPAN reads the headers from both files, and COMBO combines the receiver nodal interception matrices in some selected ratio.

HINT interpolates receiver interception data to the individual heliostat locations. A vector of receiver interception fractions is kept in core with a component for each heliostat. Similarly, an array of panel interception fractions is kept in random file 38. The linear interpolation is supported by data relating to the representative heliostats in the cellwise

performance model. It is easy to locate individual heliostats with respect to the representatives of the cell model.

CSPANL is an entry point of HINT which reads the file of individual heliostat panel fractions and converts them into circle-sector panel powers written to print and card output.

SUMIT integrates ERGM1 over the hours in a day, and ERGM2 over the days in a given year. ERGM1 is a vector of redirected energy in MWH/m^2 for the individual heliostats. Redirected power or energy includes the effect of the insolation model, diurnal motion, heliostat mounting and layout, and shading and blocking effects. However, receiver interception is not included. This subroutine assumes east-west symmetry in the collector field and morning-afternoon symmetry in insolation. If these symmetries are lacking, similar outputs for the other half field or half day can be obtained from a second application of FSAB and ASAB in YEAR.

RELPOW outputs a dimensionless measure of relative heliostat performance called RTPOW. This output is a renormalized version of ERGM1 or ERGM2 (according to whether daily or annual performance is used) such that the average of RTPOW over all heliostats equals 1. CELTUR and SECTOR outputs are also available. There are two additonal outputs which provide the "Distributions of Glass Area (and of Redirected Power) with Respect to RTPOW."

PANPOW is the last call made by YEAR. It provides annual summary output for the receiver panel powers, their statistics, and several measures of system efficiency. Any

receiver having tubes can be divided into sets of tubes called panels.

PANPOW provides the following list of outputs:

- 1) Annual Summary of Incident Panel Power
- 2) Annual Summary of Absorbed Panel Power
- 3) Annual Summary of System Efficiency
- 4) Annual Summary of System Efficiency/COSI
- 5) Annual Summary of Dimensionless Panel Gradients
- 6) Annual Summary of Receiver Asymmetry Ratios
- 7) Annual Summary of Receiver Panel Maxima printed above the Panel Number of Maxima
- 8) Annual Summary of Receiver Panel Minima printed above the Panel Number of Minima.

All of these outputs list the same set of day and hours. Items (3), (4), (6), and (7) appear as tables of day and hours, whereas items (1), (2), and (5) are lists of (day, hour) combinations in order to provide space for the output for each panel.

The absorbed panel power P_A is obtained from the incident power P_I by the linear transformation

$$P_A = aP_I - b,$$

where a and b are constants representing the multiplicative and subtractive losses of the receiver, and

a = coefficient of absorption, and

b = convective and radiative loss for specific operating conditions.

System efficiency is defined by the total redirected power absorbed by the receiver divided by the total redirected power produced by the collector field. A second measure of system efficiency is provided by dividing the total efficiency by COSI. (This removes the unavoidable cosine of incidence effect.)

The dimensionless panel power gradients $G(i)$ are defined as

$$G(i) = (P_A(i) - P_A(i-1))/(P_A(i) + P_A(i-1))$$

where $i = 1 \dots \text{NPANLS}$. The panel power maxima, panel power minima, and their locations are determined for each hour by quadratic fitting. The panel power asymmetry ratios are panel power maxima divided by panel power minima. These statistics, also provided for each hour, are useful for receiver control studies.

PANEFF is called by PANPOW in order to output under conditions of altered insolat. We are currently assuming that the insolat is $950/\text{m}^2$ at all times; however, other insolat conditons can be provided. Site specific insolat is output via PANPOW, if desired, but it could be sent to PANEFF. The following outputs are available:

- 1) Annual Summary of Incident Panel Power
- 2) Annual Summary of Absorbed Panel Power
- 3) Annual Summary of System Efficiencies
- 4) Annual Summary of System Efficiencies/COSI

SAB3 is the individual heliostat version of RSABS which is the improved shading and blocking processor for the split rectangular heliostat model.

SUBFLD redefines the collector field arrays, which are the coordinate arrays for heliostats and the interception fraction array FINT (and others), to contain data for the heliostats within specified subfield boundaries.

SECTOR generates the sector-by-sector printout of field variables for individual heliostats. SECTOR calls SECPRT to format the output print line. SECPRT in turn calls ASKPRT to insert an asterisk indicating where deletes occurred in the collector field layout process.

CELTUR may generate several possible outputs. If no print outputs are called for, CELTUR simply returns the field-variable average to the calling program. CELTUR calls CIRSEC if the CIRSEC output option is set. CIRSEC finds the field-variable average over circle sector elements and outputs the results in tabular form. In addition, CELTUR sets up the XY grid structure and calls VCONTR, which may print cell averages of the field variable in a table format depending on output switch settings, and it may also output a contour map.

5.0 Concluding Remarks

To restate the concept of the IH code in relation to the NS and RC systems, the IH system does not resort to representatives located within computational cells of the collector field like RC and NS. Actual heliostat location coordinates are used. Of course, the coordinates generated by the layout routines are developed from prior RC and CELLAY runs. IH monitors the performance of each individual heliostat, but contains no economic model and therefore does not optimize as RC does.

Currently IH does not compute images and thus must rely on the NS code for its cellwise receiver flux data. IH has detailed shading and blocking outputs for the actual field coordinates, and outputs the resulting receiver performance statistics. These can be calculated on an annual basis if desired. In conclusion, IH may be classified as a collector field layout and performance code for solar central receiver systems.